

Chapter 5 Study of electrically conductive adhesives in the manufacture of photovoltaic modules

Capítulo 5 Estudio de adhesivos conductores de electricidad en la manufactura de módulos fotovoltaicos

SORIANO-VARGAS, Orlando†*, MENDOZA-HERNÁNDEZ, Raúl, LOPEZ, Roberto and GARCIA-SANCHEZ, José Juan

TecNM/Tecnológico de Estudios Superiores de Jocotitlán, Carretera Toluca Atlacomulco km 44.8, Ejido de San Juan y San Agustín, Jocotitlán, México

ID 1st Author: *Orlando, Soriano-Vargas* / **ORC ID:** 0000-0002-9331-7909

ID 1st Co-author: *Raúl, Mendoza-Hernández* / **ORC ID:** 0009-0003-7169-6551

ID 2nd Co-author: *Roberto, López-Ramírez* / **ORC ID:** 0000-0001-8341-3684

ID 3rd Co-author: *Jose Juan, García-Sánchez* / **ORC ID:** 0000-0002-6415-7854

DOI: 10.35429/H.2023.5.61.85

O. Soriano, R. Mendoza, R. López and J. García

*orlando.soriano@tesjo.edu.mx

R. López (AA.) Engineering and Architecture in the Northern part of the State of Mexico. Handbooks-TI-©ECORFAN-Mexico, Estado de México, 2023

Abstract

In this work, the behavior of an electrically conductive adhesive (ECAs) was selected and studied, using shingled technology is a development in the connection of solar cells by means of superimposition with electrically conductive adhesives, thus obtaining higher powers than the previous welding process, also offers several advantages compared to standard photovoltaic modules, improving: efficiency, reduction of microcracks, better use of the surface, lower processing temperature, higher energy yield, and better aesthetics.

The objective of this study was to analyze electrically conductive adhesives for use in the manufacture of photovoltaic modules to propose a technological development to obtain greater efficiency in energy capture. Polycrystalline cells and monocrystalline cells were studied. The photovoltaic module manufacturing set was made using the conventional fixing method to join solar cells, based on the union by welding with Sn-Cu connection tapes. Loctite Ablestik ICP 8282 adhesive was selected for use in the manufacture of the overlay prototype and the substitution of the welding process in the manufacture of standardized photovoltaic modules. The adhesive curing consisted of depositing the joined cells, in the Stringer equipment, for 30 seconds at a temperature of 150°C.

The Shingled prototype went through the lamination process where the temperature was raised to 150 °C for 15 minutes for polycrystalline cells and monocrystalline cells. 5 modules were studied by the electroluminescence test showing defects such as cracks in the manually manufactured modules. Modulo 5 was acceptable because a homogeneous image is shown in each of its cells on the union by dosage, thus giving a figure free of microcracks and any other defect. The photovoltage test was a notable difference in module 5 its high efficiency of 20.90% that other. The shadow moment testing in modules 1 and 5 connected with electrically conductive adhesives are better because they have lower percentages in the presence of a clogged cell.

However, when we change the 20% shadow angle on each module, we will have a total loss in power and efficiency in modules 2 and 3. Thermographic performance shown the module 5 is a reference of the objective to be achieved with the use of the electrically conductive adhesive, but it did not obtain any loss of power or efficiency.

Electrically conductive adhesive, shingled technology, polycrystalline cells, monocrystalline cells

Resumen

En este trabajo se seleccionó y estudió el comportamiento de un adhesivo eléctricamente conductor (ECAs), utilizando la tecnología shingled es un desarrollo en la conexión de células solares mediante la superposición con adhesivos eléctricamente conductores, obteniendo así potencias superiores al proceso de soldadura anterior. También ofrece varias ventajas respecto a los módulos fotovoltaicos estándar, mejorando: eficiencia, reducción de microfisuras, mejor aprovechamiento de la superficie, menor temperatura de procesamiento, mayor rendimiento energético y mejor estética.

El objetivo de este estudio fue analizar adhesivos eléctricamente conductores para su uso en la fabricación de módulos fotovoltaicos para proponer un desarrollo tecnológico para obtener una mayor eficiencia en la captura de energía. Se estudiaron células policristalinas y células monocristalinas. El conjunto de fabricación del módulo fotovoltaico se realizó mediante el método de fijación convencional para unir células solares, basado en la unión mediante soldadura con cintas de conexión de Sn-Cu. Se seleccionó el adhesivo Loctite Ablestik ICP 8282 para su uso en la fabricación del prototipo de superposición y la sustitución del proceso de soldadura en la fabricación de módulos fotovoltaicos estandarizados. El curado del adhesivo consistió en depositar las células unidas, en el equipo Stringer, durante 30 segundos a una temperatura de 150°C.

El prototipo Shingled pasó por el proceso de laminación donde la temperatura se elevó a 150 °C durante 15 minutos para células policristalinas y células monocristalinas. Se estudiaron 5 módulos mediante la prueba de electroluminiscencia mostrando defectos como grietas en los módulos fabricados manualmente. El módulo 5 fue aceptable porque se muestra una imagen homogénea en cada una de sus celdas sobre la unión por dosificación, dando así una figura libre de microfisuras y cualquier otro defecto.

En la prueba de fotovoltaaje se observó una diferencia notable en el módulo 5 por su alta eficiencia del 20,90% respecto a los demás. Las pruebas de momento de sombra en los módulos 1 y 5 conectados con adhesivos eléctricamente conductores son mejores porque tienen porcentajes más bajos en presencia de una celda obstruida. Sin embargo, cuando cambiamos el ángulo de sombra del 20% en cada módulo, tendremos una pérdida total de potencia y eficiencia en los módulos 2 y 3. El rendimiento termográfico mostrado en el módulo 5 es una referencia del objetivo a conseguir con el uso del adhesivo eléctricamente conductor, pero no obtuvo ninguna pérdida de potencia o eficiencia.

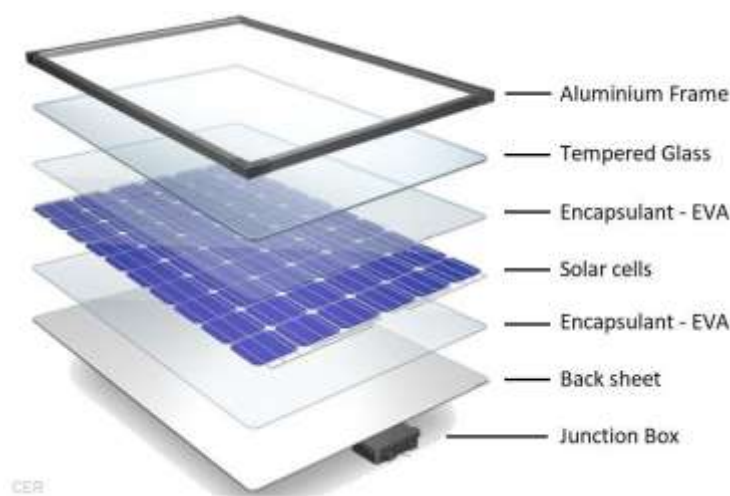
Adhesivo eléctricamente conductor, Tecnología shingled, Células policristalinas, Células monocristalinas

1. Introduction

1.1 Photovoltaic module

The photovoltaic module can be defined as a set of elements represented in figure 1, which convert solar energy into electrical energy through solar cells.

Figure 1 Structure of the components that make up a photovoltaic module



Source ([Svarc 2020](#))

1.1.1 Cell types

Monocrystalline: Cells cut from a single crystal of Silicon, are more efficient.

Polycrystalline: Cells cut from a block of silicon composed of many crystals.

1.2 Electrically Conductive Adhesives (ACE)

Electrically Conductive Adhesives (ACE) are prepared from an insulating polymeric matrix that provides adhesion and resistance, while a metallic filler is responsible for conducting electricity. To become a hybrid, different methods are used, such as doping with other components. Being connection materials that can be used to facilitate a mechanical coupling and an electrical connection (Springer and Bosco 2020).

1.2.1 Bonding material

The bonding material used are polymers of different compositions and reactive groups, epoxy is the most used material as an adhesive, being a thermosetting polymer (Springer and Bosco 2020).

1.2.2 Backfill material

The filler material is metallic elements on a nanometric scale, such as: silver, gold, and copper where you can find two types of conductive adhesives divided by their morphology and percentage of metallic filling (Springer *et al.* 2020). There are three different fill geometries in the form of spheres, lamellae, and holes.

1.3 Types of Electrically Conductive Adhesives (ACE)

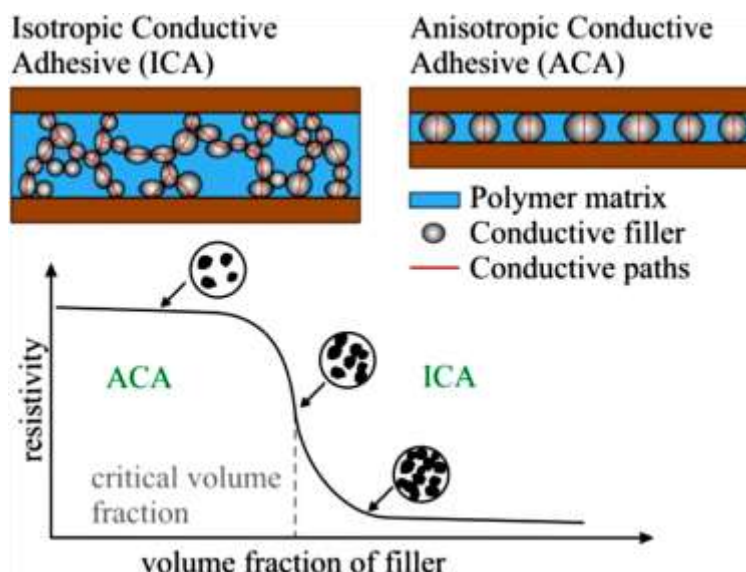
1.3.1 Isotropic Conductive Adhesives (ACI)

Isotropic adhesives consist of approximately 70-80% metal particles, when the adhesive cures the particles are evenly distributed and form a network within the polymer structure, allowing current flow in three directions (X, Y and Z) (Sharma *et al.* 2021).

1.3.2 Anisotropic Conductive Adhesives (ACA)

They are electrical conductors in only one direction, this directionality of the electrical property is called anisotropy. Anisotropy occurs when the polymer chains are oriented in the direction of flow. This directional conductivity is achieved by using a relatively low volume of metal filler well below the percolation point (5-10% volume) (Malik *et al.* 2021) Next, in figure 2 the structure of the two types of electrically conductive adhesives is shown.

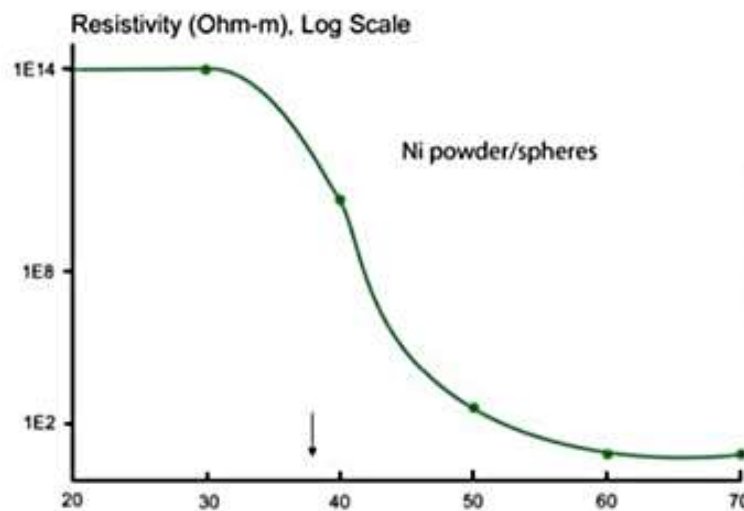
Figure 2 Structural comparison of rates ACE



Source (Pander *et al.* 2014)

1.4 Percolation Theory

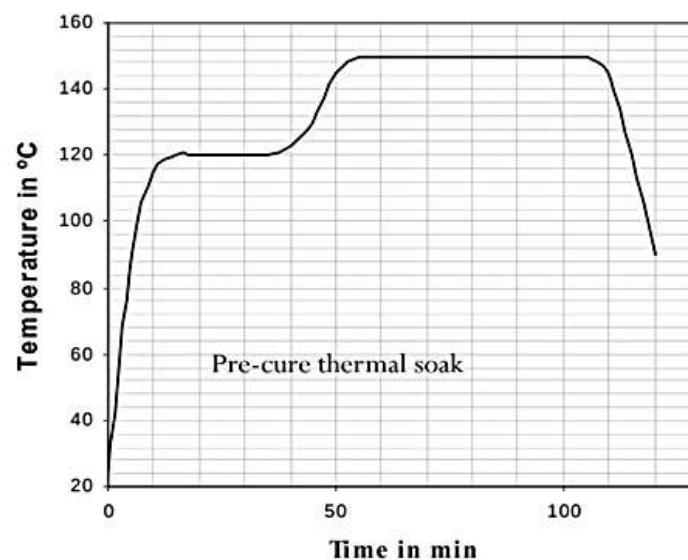
Percolation theory dictates a "critical" concentration on the metal filler at which a three-dimensional lattice and conductivity is established. Thereafter, the conductivity slowly changes with increasing metal filler concentration as can be seen in figure 3. The percolation point is reached when enough metal filler has been loaded into the polymer to transform the compound from an insulator to a conductor. In Anisotropic Conductive Adhesives, they have low volume metal fillers (typically 5-10% by volume). This is as opposed to Isotropic Adhesives (ACI), they typically have a higher amount of filler than is needed to reach the set point, approximately 70-80% (Pander *et al.* 2014).

Figura 3 Teoría de la percolación, % concentración

Source (Pander *et al.* 2014)

1.5 Curing Process

Figure 4 shows the schematic of the curing process, include exothermic reactions that convert monomers or pre-polymers in a liquid state into a three-dimensional network. Incomplete curing will result in weak adhesion, while over-curing can cause bond degradation (Elsayed *et al.* 2020).

Figure 4 Step of curing process

Source (Anderson *et al.* 2021)

1.6 Classification of electrically conductive adhesives (ECA)

1.6.1 Epoxy

Most epoxy adhesives contain Diglycidyl Ether of Bisphenol A (DGEBA) as the main epoxy resin base. Epoxy resins are very versatile structural adhesives because they can react together with many different resins and low molecular weight compounds (Saedi *et al.* 2022). Silver-filled epoxy adhesives provide a high-strength conductive bond. Its properties are: (such as cohesive strength, hardness, toughness, flexibility, chemical, electrical, and mechanical resistance) (Guo *et al.* 2023).

1.6.2 Silicones

Silicones are hybrid compounds that combine the function of a reactive organic group with the inorganic characteristic of an alkyl silicate, in one. The high flexibility of the silicone chain is due to the low rotational energy barrier of the Si-O bond. Electrically conductive silicone adhesives with graphite fillers are often used for antistatic systems. These materials are generally very high in viscosity and thick in consistency, making them suitable for large area bonding. An important feature to keep at a temperature (-20 °C) (Guo *et al.* 2023).

1.6.3 Polyurethane

Polyurethane adhesives have properties such as: rigid, hard, flexible, and soft. Silver-filled polyurethane adhesives are two-part adhesives, so they require mixing or are supplied pre-mixed like epoxies. They offer high peel strength and flexibility. Since they are filled with silver, high levels of conductivity can be achieved (around 0.0001 Ω/cm to 0.0004 Ω/cm) (Guo *et al.* 2023).

1.6.4 Acrylates

Acrylic adhesives are thermosetting systems, also called reactive acrylics. They are liquids with low viscosity that reach polymerization faster with less time before exposure to temperature, forming resistant bonds. Most thermosetting acrylic adhesives are two-part systems that provide shear strength (Guo *et al.* 2023).

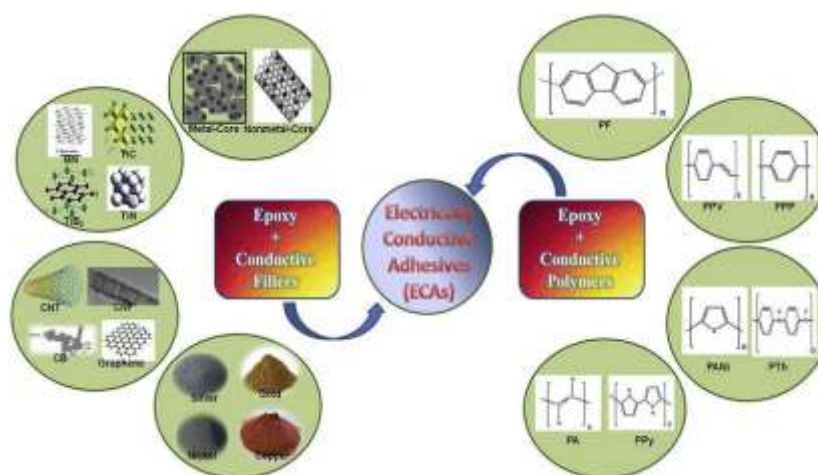
1.6.5 Bismaleimide

Bismaleimide (BMI) adhesives are used in the manufacture of printed electronic flexible circuits and other electronic devices, as well as in applications where resistance to high temperatures is required. As one of the most important mechanical properties is traction. Being suitable for long-term exposure to temperatures up to 200 °C and for short-term exposure up to 230 °C (Malik *et al.* 2021).

1.6.6 Hybrids

Adhesives composed of two or more types of electrically conductive adhesives. Next, in figure 5 the classification of ECAs is represented.

Figure 5 Classification of electrically conductive adhesives



Source (Aradhana *et al.* 2020)

1.7 Properties of electrically conductive adhesives

Electrical conductivity and bond strength are electrical properties of electrically conductive adhesives.

1.7.1 Electrical conductivity

Electrical conductivity is a transport phenomenon in which electrical charge (in the form of electrons or ions) moves through a system. Electrically conductive adhesives have a low conductivity before the curing process. This conductivity increases after the contraction of the adhesive, increasing the contact between the particles of the metallic filler. However, although thermosetting materials shrink slightly upon curing, excessive shrinkage can cause bond failure (Springer and Bosco 2020).

1.7.2 Strength of joints

The resistance of the joints is a characteristic property that will depend on the connection and the metallic elements in the bases that are assembled.

1.7.3 Cohesive force

The cohesive strength of an ECAs refers to the internal strength of the adhesive, which depends on the type of polymer used and the amount of metal filler present. It can be shown that a large amount of metal filler within the adhesive reduces the bond strength. Conversely, a reduction in metal filler will improve cohesive strength, but reduce electrical conductivity.

1.7.4 Bond adhesion strength

The adhesion force of a conductive adhesive refers to the adhesion force between the bases. Thermosetting materials, such as epoxy, have a higher bond strength than thermoplastics. Thermosetting polymers can produce both strong covalent and secondary bonds, whereas thermoplastics can only form secondary bonds (Springer and Bosco 2020).

1.8 Other factors that increase joint strength include.

1.8.1 Corrosion

Corrosion is a process that occurs under humid conditions in the presence of an electrolyte and is most prominent in high moisture absorption adhesives. The material with the highest electrochemical potential is ACE epoxy, which acts as the cathode and the base of the cell acts as the anode. During the electrochemical process, the anode corrodes (Springer and Bosco 2020).

1.9 Use of conductive adhesives as a replacement for solder

It is necessary to define the electrical and mechanical properties of electrically conductive adhesives (ACE), for substitution (Springer and Bosco 2020).

1.9.1 Electrical requirements.

Volume resistivity is the electrical resistance of a body whose length and area uniform cross section (Springer and Bosco 2020):

- Volumetric resistivity less than 0.001 Ohm/cm³.
- Displacement of joint movement less than 20%.

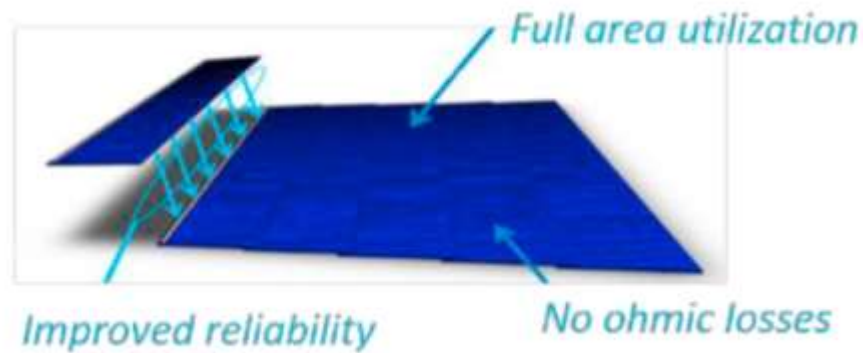
1.10 Overlay Technology

Overlay technology is a technological advance used to obtain a power increase, this technique eliminates the need for Sn-Cu connection tapes by 90% and therefore reduces resistance losses. The main difference with other techniques is the efficiency, aesthetics, and performance of the overlay photovoltaic modules.

The development of superimposition technology, implies the superposition of the cells, increasing the ratio between the limit of the cell and the area thereof, one on top of the other with an electrically conductive adhesive, the main advantage of which is an increase in the energy production, due to more efficient packing between the cells (Tonini *et al.* 2018).

For correct operation, the screen printing of each cell must follow the scheme, where there is a correct connection with the adhesive in the overlap, figure 6 shows how the screen printing of a cell should be.

Figure 6 Shingling interconnection scheme

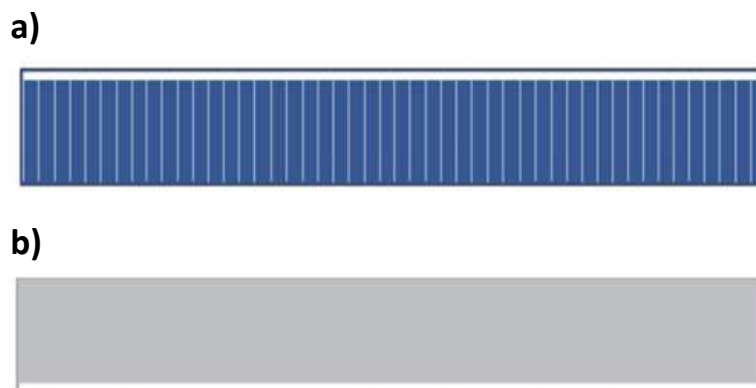


Source (Tonini et al. 2018)

1.10.1 Design of the cells

The cells must have a BUS-BAR (energy collector bar) along the edge, one at the front and one at the back as shown in figure 7, with cell dimensions $(156 \text{ mm} \times 31 \text{ mm}) \pm 0.1 \text{ mm}$ (Oh et al. 2020)

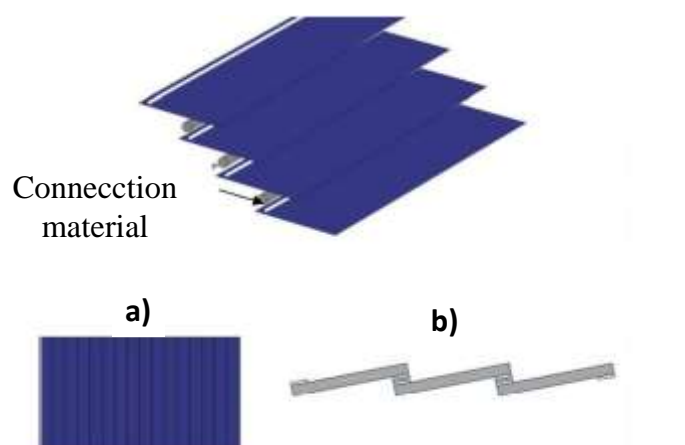
Figure 7 Design of a cell (a) Top View (b) Bottom View



Source (Beaucarne 2016)

To form a string (set of cells placed one on top of the other), the electrically conductive adhesive (ACE) dosing process is carried out, connecting the rear BUS-BAR with the next front cell as shown in the following figure. 8.

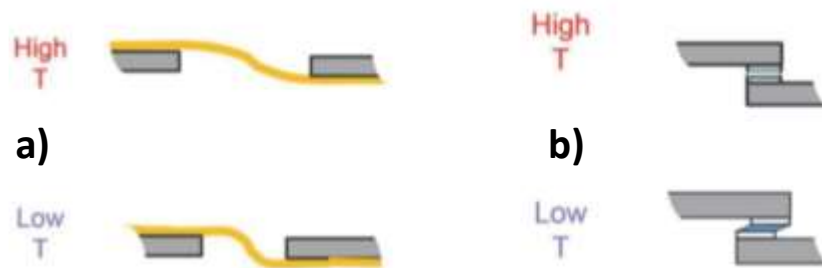
Figure 8 Design of a string (a) Top view of a string (b) Cross sectional view.



Source (Beaucarne 2016)

To verify its effectiveness absorbing tensions, a thermo-mechanical situation of two cells that are stimulated towards each other is assumed, section A was through the Sn-Cu welding process and simultaneously applying an increase in temperature where they will deform slightly allowing movement. Item B was carried out with the overlapping connection of the electrically conductive adhesives, the movement of the cell is much more limited and the joints between the cells tend to allow movement due to deformation while supporting mechanical stress as shown in the figure. 9.

Figure 9 Thermo-mechanical representation of the different connections (a) Deformation of the Sn-Cu welding process; (b) Deformation of the overlap joint

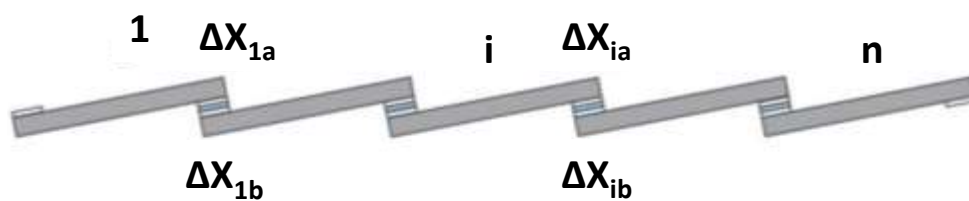


Source (Beaucarne 2016)

1.10.2 Structure

Figure 10 shows the structure of the string in the form of an overlap in a cross-sectional section. There are n cells and therefore $n-1$ junctions.

Figure 10 Structure of the overlay model, cross-sectional cut



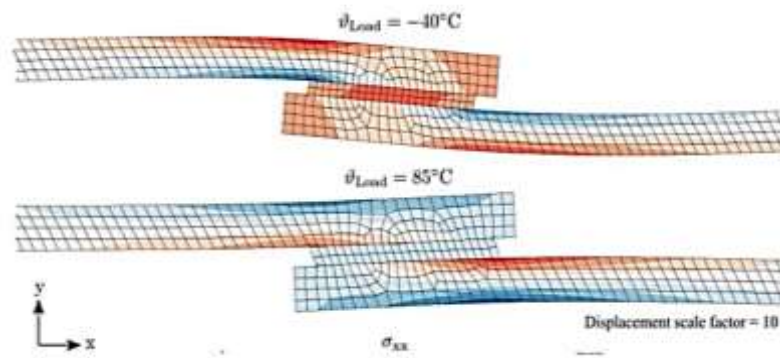
Source (Beaucarne 2016)

The junctions will form at 150 °C, it should be noted that if the string is cooled to -40 °C the silicon cells contract slightly. Because it is uncontrollable, the movement will not be opposed and there will be no mechanical stress.

1.10.3 Structural deformation of a connection by using ACE.

Complementing with the previous analysis of the effectiveness absorbing tensions, a simulation of deformation was carried out in the joints of two substrates with the application of an adhesive conductor of electricity, the first test was at a temperature of -40 °C where the deformation tends to contract, in the second test the application temperature was 85 °C, in which the stresses remain stable providing a favorable point of view to the photovoltaic modules as can be seen in figure 11, when they are exposed to different temperatures so as not to cause defects in the joints (Springer and Bosco 2020).

Figure 11 Structural deformation of a connection between an electrically conductive adhesive and two adjacent silicon cells for two different charging temperatures



Source (Springer and Bosco 2020)

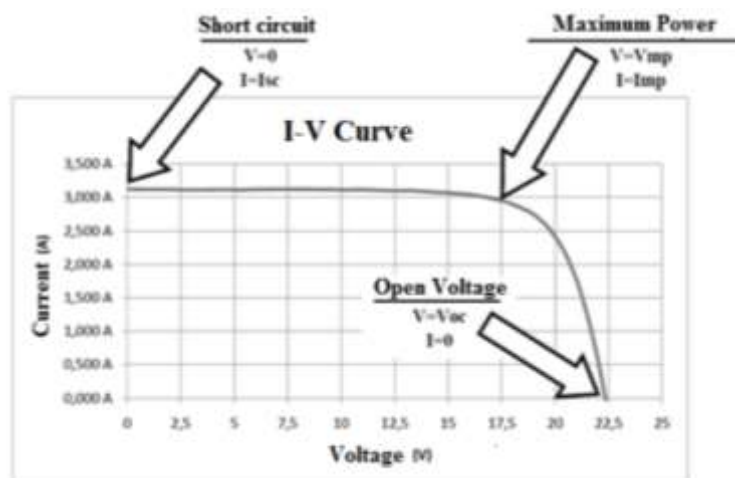
1.11 Electroluminescence

Electroluminescence (EL) solar cell imaging relies on the same principle as a light emitting diode (LED), where a source of current is provided into a solar cell and radiative recombination of emitted carriers causes a light emission. As an indirect bandgap semiconductor material, the peak of carrier recombination in silicon occurs through defected locations (Dhimish and Holmes 2019).

1.12 I-V curve

In the I-V curve (figure 12) can extract the electrical characteristics of the photovoltaic cell in standard conditions of measurement (SCM): ISC (short circuit current) is maximum intensity that can generate a photovoltaic cell or module when measuring the current if performing a short circuit (output voltage of 0 volts), VOC (open circuit voltage) is maximum voltage that can generate a photovoltaic cell or module when measuring the voltage if not flowing current (current of 0 amps), P_{MAX} (Maximum power) is maximum power that can generate a photovoltaic cell or module and it's the product of maximum voltage and current, V_{MAX} (Maximum Voltage) is the voltage at maximum power (around 80% of open circuit voltage) and I_{MAX} (Maximum Current) is the current at maximum power (Aparicio *et al.*, 2013)

Figure 12 Representation of an I-V Curve



Source (Aparicio *et al.*, 2013)

2. Methodology

2.1 Materials

Table 1 compares the 10 conductive adhesives. The adhesive "Loctite Ablestik ICP 8282" was selected for use in the manufacture of the overlay prototype and the substitution of the welding process in the manufacture of standardized photovoltaic modules. This adhesive has a resistance of 0.0037 Ohm/cm³, its time and temperature in the curing process it is 30 s at 150 °C. Being a single-component acrylate type adhesive, it does not need to be mixed with other additives. Too, the adhesive was based on commercial availability and in-stock at the company.

2.2 Overlay prototype

The overlay prototype was made by joining together 44 monocrystalline silicon cells with dimensions (156mm x 39mm). Obtaining these half cells was carried out by cutting an entire cell in two, by means of a laser cut. It should be noted that the process of cutting the half cells is a fragile process because it can generate fissures or microcracks.

2.3 Preparation of the Henkel Loctite 98666.




The dispensing equipment was connected to a compressor. adjusting the pressure to 500 kPa for the dosing of the adhesive, which was applied manually (figure 13). To obtain the volume of each application we will use the following equation1 of the cylinder, where we take as reference the internal radius of the dispensing needle (0.010") times the length of the cell and the calculated volume is 0.31 mL. The nozzle is cleaned each time it is used to avoid contamination and material buildup. The conservation of the material must be at a temperature of (-20 °C) this to avoid any possible polymerization.







Figura 3 Dosification process



Source (Own Elaboration)

Table 1 Comparison of the properties of ACE electrically conductive adhesives

Imagen	Type	ACE	Resistance Ohm/cm ³	Force shear N/mm ²	Cured °C	Thermal Conductivity W/(m·K)	Stock temperatura °C	Supplier
	8282	Acrylate	0.0037	9.1	0.5 min a 150 °C	-	-20 °C	Henkel
	SC10	Epoxi	0.0040	6	0.5 min a 180 °C	-	-20 °C	Heraeus
	8311	Acrylic	0.00039	11.4	0.16 a 0.25min a 150 °C	-	-20 °C	Henkel

	9410	Epoxi	0.0018	26	7 min a 120 °C	1.1	22 °C	Mg Chemicals
	QMI 529HT- LV	BMI	0.00005	20	30 min a 175 °C	8	-40 °C	Henkel
	3888	Epoxi two	< 0.001	12	60 min a 150 °C	1.5	-	Henkel
	56C	Epoxi two	0.0004	6	120 min a 50 °C	3	-	Henkel
	EC- 6601	Silicona	0.0027	1.61	30 min a 60 °C	2.12	-	Dowsil
	8331S	Epoxi two	0.006	65	40 min a 100 °C	1.3	-	Mg Chemicals

Source (Own Elaboration)

2.4 Preparation of the curing process

Considerations that must be considered to carry out the curing process, the aluminum base where the strings will be made, had a preheating of 25 °C to avoid a thermal shock when passing through the Stringer device "SOMOT" illustrated in figure 14. The Adhesive curing consists of depositing the joined cells, in the Stringer equipment, for 30 seconds at a temperature of 150 °C. This ensures the solidification of the adhesive, checking the temperature with an infrared thermometer.

Figure 14 "SOMOT" Stringer equipment and an Infrared thermometer



Source (Own Elaboration)

In each application of each cell on the string, an inspection of the surface was carried out looking for visible defects in the superimposition of the cells, for example: broken cells, narrow spaces in the strings. Subsequently, the curing process in each cell exposed to a constant temperature of 150 °C for 30 seconds.

Each string consisted of 10 dosages, the superimposition was made taking care of the integrity of the half cells, in total 4 strings with 11 monocrystalline half cells were obtained, as can be seen in figure 15.

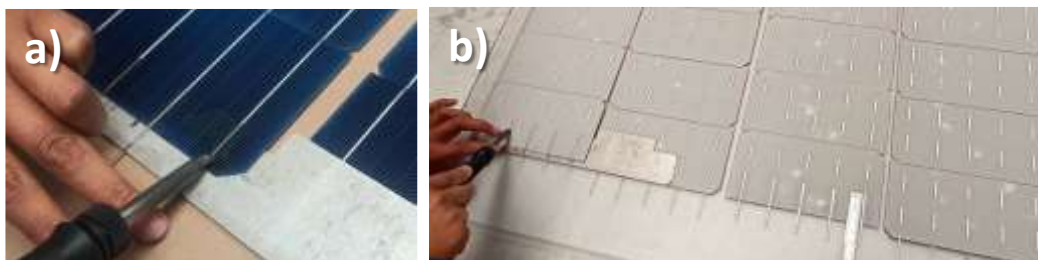
Figure 15 Formation of 4 strings

Source (Own Elaboration)

2.5 Assembly

The assembly procedure began by cutting transparent EVA back sheets and EVA encapsulants of (980 x 660) mm each, then the extra clear tempered glass of (970 x 654) mm is placed, later an EVA encapsulant sheet aligning all the components. The strings are then incorporated, maintaining a 2 mm separation between each string. For the Shingled prototype, 4 strings of 11 cells were needed, joining the connections to close the series circuit. For this step, Sn-Cu interconnection tapes with dimensions of 1 x 50 mm were cut, each string has a geometry of 5 Bus-Bar by end, we begin with the union of the Sn-Cu interconnection tapes by means of the union by the welding process in each Bus-Bar, Flux solution was applied to each weld at a height of 25 mm, with in order to eliminate oxides present in the component and have a better handling in the soldering station, at a temperature of 370 ± 5 °C. The connection in series begins on the negative side, the next string will begin the connection on the positive side of the cell, see figure 16. In the welding process, the components of the prototype are protected with a "Mecanitec" non-stick tape, this tape insulates the temperature so as not to melt transparent EVA back sheets.

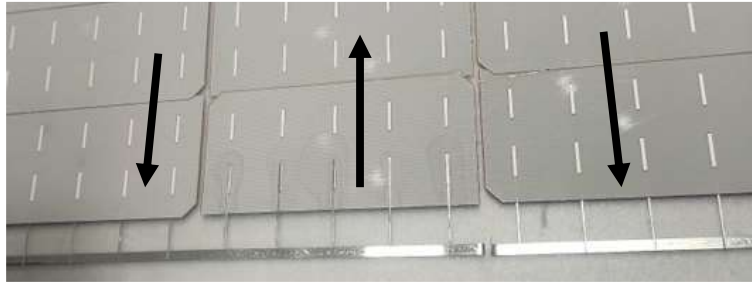
Figure 16 a) Use of "Mecanitec" anti-adherent tapes in each joint by welding, and b) join of the Sn-Cu interconnection tapes at the end of each string



Source (Own Elaboration)

Figure 17 shows Sn-Cu connection tapes, (6x350) mm, and (6x290) mm, were used to close the circuit of the photovoltaic module with positive and negative terminals. We placed another EVA encapsulating sheet and a white EVA back sheet.

Figure 17 Orientation of the strings and closure of the photovoltaic module circuit



Source (Own Elaboration)

2.6 Lamination process

The Shingled prototype went through the lamination process where the temperature was raised to 150 °C for 15 minutes, melting sheets of EVA (Ethyl-Venil-Acetate), thus encapsulating the components, later the prototype advanced to the area where 4 fans are located to cool the module for 10 minutes. Immediately transported the module on a table to remove the excess of the fused EVA back sheets with isopropyl alcohol removing traces of the molten polymer, the finished prototype can be seen in figure 18.

Figure 18 Shingled prototype assembled



Source (Own Elaboration)

2.7 Monocrystalline photovoltaic module (welding).

A photovoltaic module was made with the same monocrystalline cells, but with the standard process in the manufacture of conventional photovoltaic modules, production began by placing tempered glass (1050 x 670) mm, later an EVA encapsulating sheet was placed as illustrated in the figure 19.

Figure 19 Placement of a transparent EVA backsheet



Source (Own Elaboration)

For this test photovoltaic module, 4 strings of 12 half cells were needed, joining the half cells by the welding process, cutting Sn-Cu interconnection tapes with dimensions 1 x 50 mm for the length of each Bus-Bar, in each string has a geometry of 5 Bus-Bar per end, it begins with the union of the Sn-Cu interconnection tapes applying the Flux solution in each union by the welding process at a height of 25 mm, in order to eliminate oxides present and have a better handling in the soldering station, at a temperature of $370\text{ }^{\circ}\text{C} \pm 5\text{ }^{\circ}\text{C}$ (see figure 20). For the series circuit, the union began on the negative side, later for the next string the union will be on the positive part of the cell. In the soldering station, the components of the prototype are protected with a “Mecanitec” non-stick tape, it is isolated from the temperature so as not to melt the encapsulant EVA. Figure 25 Sn-Cu connection tapes, (6x350) mm and (6x290) mm, were used to close the circuit of the photovoltaic module.

Figure 20 Joining process of monocrystalline cells by means of the soldering station



Source (Own Elaboration)

2.8 Monocrystalline Lamination process

The Shingled prototype went through the lamination equipment, where the temperature was raised to $150\text{ }^{\circ}\text{C}$ for 15 minutes until the EVA (Ethyl-Venyl-Acetate) encapsulants melted to fix the components. Afterwards, the photovoltaic module is cooling for 10 minutes. The photovoltaic module was immediately cleaned with isopropyl alcohol, removing traces of the molten polymer (see figure 21).

Figure 21 Assembled monocrystalline photovoltaic module (by welding)

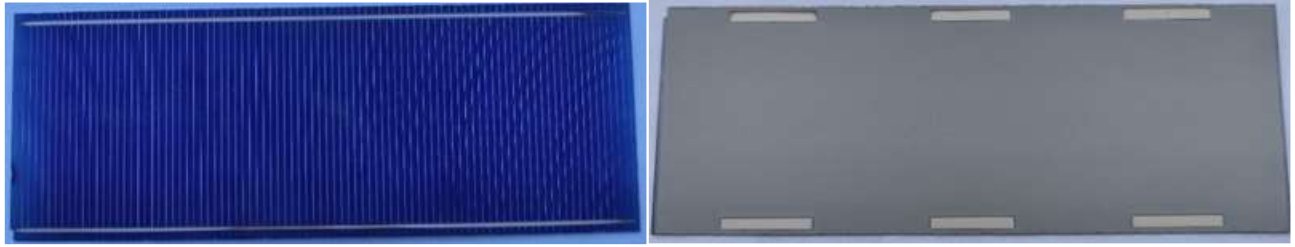


Source (Own Elaboration)

2.9 Polycrystalline shingled photovoltaic module

The preparation of this photovoltaic module was carried out with polycrystalline cells cut with dimensions (28x150) mm, see figure 22. The system is made up of 80 cells distributed in 4 strings.

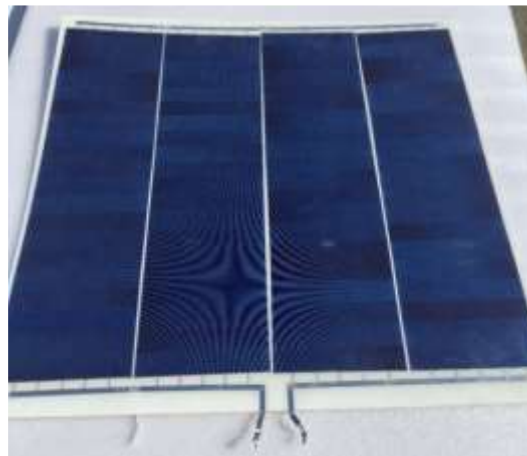
Figure 22 Polycrystalline cell (28x150) mm



Source (Own Elaboration)

The same assembly process of the Shingled prototype was used in this photovoltaic module, see figure 23. The union of the polycrystalline cells was with different dimensions, and a transparent EVA sheet was used. The photovoltaic module has a dimension (650x630) mm.

Figure 23 Shingled polycrystalline photovoltaic module

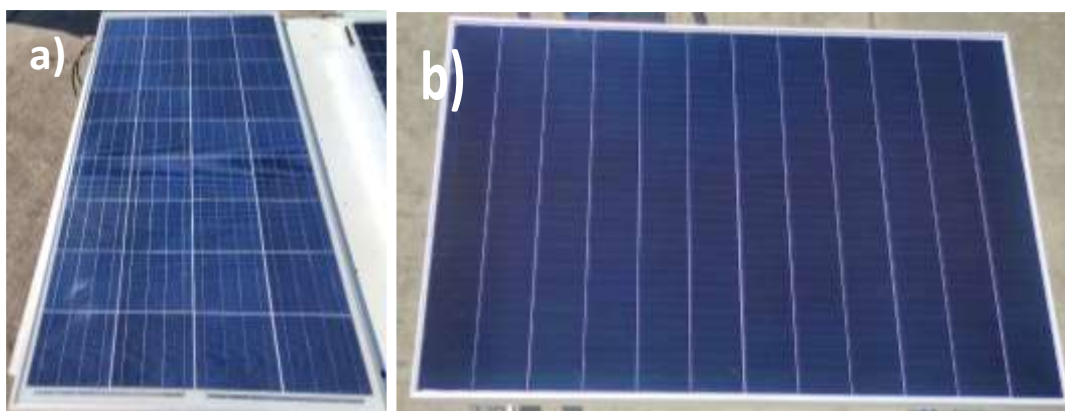


Source (Own Elaboration)

2.10 Polycrystalline photovoltaic module 120 W and monocrystalline shingled 375 W

Through the management, it was possible to obtain two photovoltaic modules by donation: a polycrystalline 120 W and a monocrystalline shingled 375 W (figure 24). The photovoltaic modules were manufactured in an automated system with the highest quality control.

Figure 24 Photovoltaic module a) 120W polycrystalline, and b) shingled 375W monocrystalline



Source (Own Elaboration)

2.11 Electroluminescence testing

The experimental modules were tested by electroluminescence and IV (under STC condition). Then, the module was put into the steady-state box, with the irradiance of $1000\pm 50\text{W/m}^2$, the temperature of $60\pm 5^\circ\text{C}$.

2.12 I-V Testing

Using a Solmetric PV analyzer I-V, the current density-voltage (J-V) curves of the PSCs were recorded from a solar simulator (AM1.5G, 1000mW/cm^2 , K). By means of the equipment "PV Analyzer I-V Curve Tracer" shown in figure 39, data on yields were obtained. The equipment allows knowing the effective power of each photovoltaic module under different climatic conditions at the different irradiation points of the day. This calculation can have significant variations, especially when the module is dirty, damaged or in unfavorable weather.

2.13 Thermographic testing

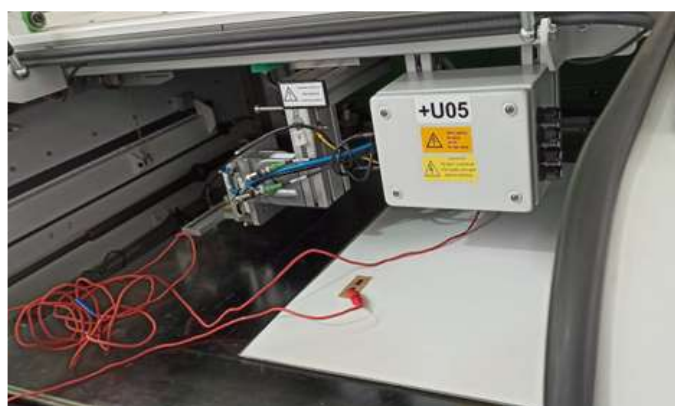
The thermographic inspection allows us to detect points of overheating, and existing broken cells in the photovoltaic modules. The camera provides a resolution of 384×288 pixels with a wide scale measurement over temperature, plus a spectral range parameter. Photovoltaic modules work in a temperature range not greater than 80°C . High temperatures directly impact photovoltaic modules presenting overheating, causing a drop in each aspect to be evaluated. Some additional parameters in this analysis are having a minimum distance of one meter in each inspection, its field of vision must have an inclination of 25° , and the working temperature in the photovoltaic modules must not exceed 80°C .

3. Results and Discussion

3.1. Electroluminescence test

In this test, the inspection of the photovoltaic modules was carried out in the cabin, in which the terminals were connected, see figure 25, inducing an electric current of 4.5 A to expose the defects (microcracks) in each module. The non-visible spectral response has a great variety between the polycrystalline and monocrystalline cell. The spectral response for polycrystalline PV modules is needed from 600-800 nm, however, for monocrystalline PV modules it is required from 1000-1200 nm.

Figure 25 Electroluminescence inspection system



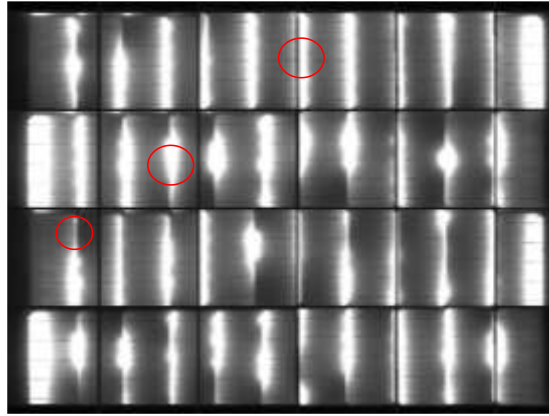
Source (Own Elaboration)

The results between each photovoltaic module are notorious, the first inspected module 1 presents luminous areas, (see figure 26), this is mainly due to the manufacturing procedure. Two main inconsistencies were deduced:

- The cut of the cells must conform to the structure of the Bus-Bar (see figure 7).
- In the dosage it presents uniformity of the adhesive.

It should be noted that the connection was not correct, however, there were no cracks or broken cells due to the dosing process.

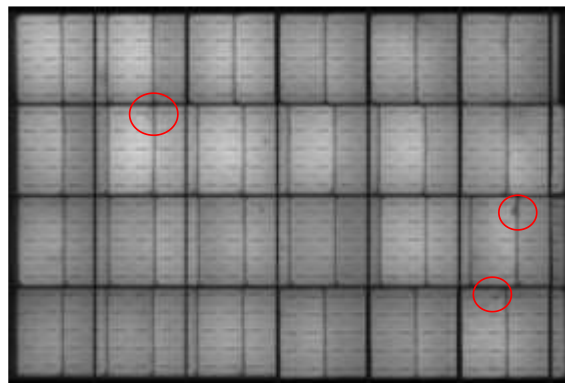
Figure 26 Electroluminescence testing: Module 1



Source (Own Elaboration)

In figure 27, the module 2 shows a homogeneous image, without change, but in the areas marked in red there are cracks and broken cells due to the welding process.

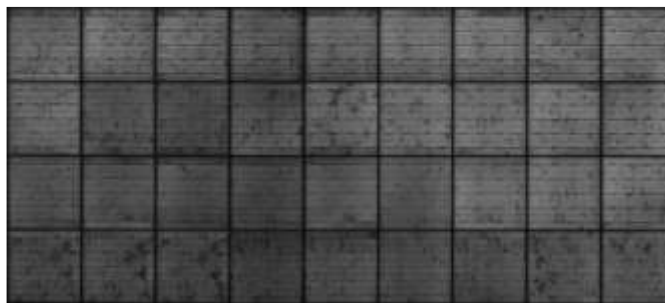
Figure 27 Electroluminescence testing: Module 2



Source (Own Elaboration)

Figure 28 shows a darker appearance with variations in the luminosity intensities, this is due to its composition of the polycrystalline cell, which is made up of small crystals, with an efficiency of approximately 25% compared to monocrystalline cells.

Figure 28 Electroluminescence testing: Module 3



Source (Own Elaboration)

Module 4 was made with polycrystalline cells using Shingled technology. No image was obtained in the electroluminescence test due to its low current caused in the laser cutting process, fracturing a large part of the cell as can be seen in figure 29. Module 4 was manufactured with great care, but without tempered glass it was replaced by a transparent EVA sheet instead.

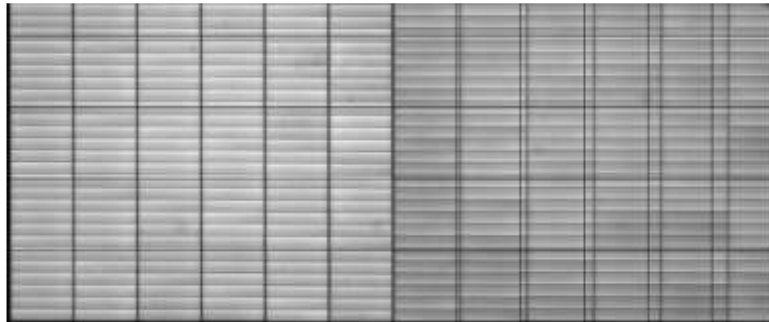
Figure 29 Polycrystalline cell damaged by the laser cutting process



Source (Own Elaboration)

The last figure of this test is from module 5, which was acquired for analysis in the production area. The results were acceptable because a homogeneous image is shown in each of its cells on the union by dosage, thus giving a figure free of microcracks and any other defect (see figure 30).

Figure 30 Electroluminescence testing: Module 5

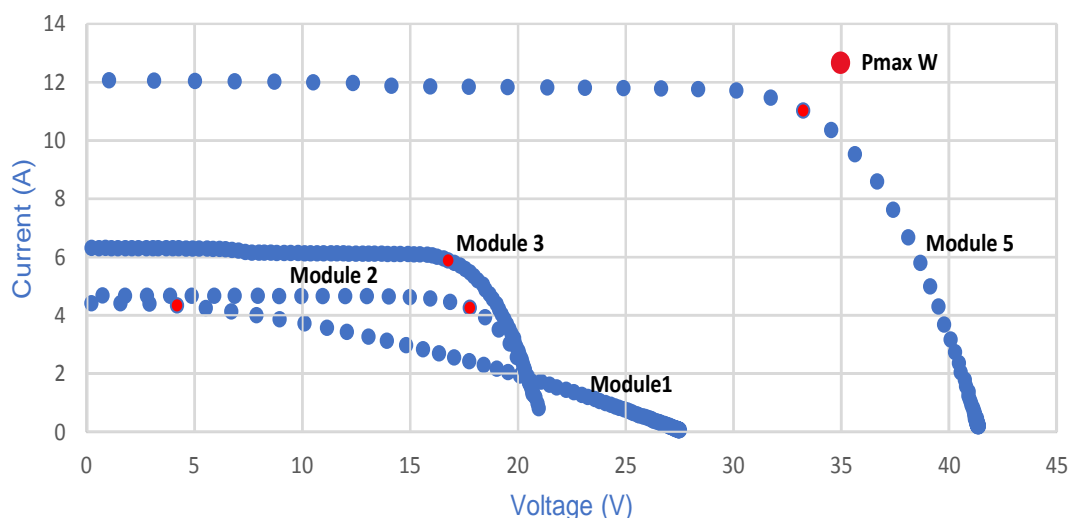


Source (Own Elaboration)

3.2 Photovoltaic performances

Figure 31 show the I-V curve of the module 1, 2, 3 and 5. The I-V curve represents the values of intensity on the Y axis and voltage on the X axis. These tests were executed more than 10 times at each recorded time. Evidencing the instability of the module 1 as in the electroluminescence test. The module obtained a maximum power of 44 W with an efficiency of 3.49%. In the I-V curve of module 2, the improvement in its performance is notorious, due to the correct union in the welding union process. The fall of the curve is prolonged at the point of maximum power. The values reached in Pmax (W) were 101.2 W with an efficiency of 8.21 %. For module 3, the value of the maximum power obtained was 99.6 W with an efficiency of 12.67%. A notable difference in module 5 is its high efficiency. With a maximum power reaching 378 W and an efficiency of 20.90%. Li *et al.*,1997., mentioned the average efficiency has a parameter of 15–17%.

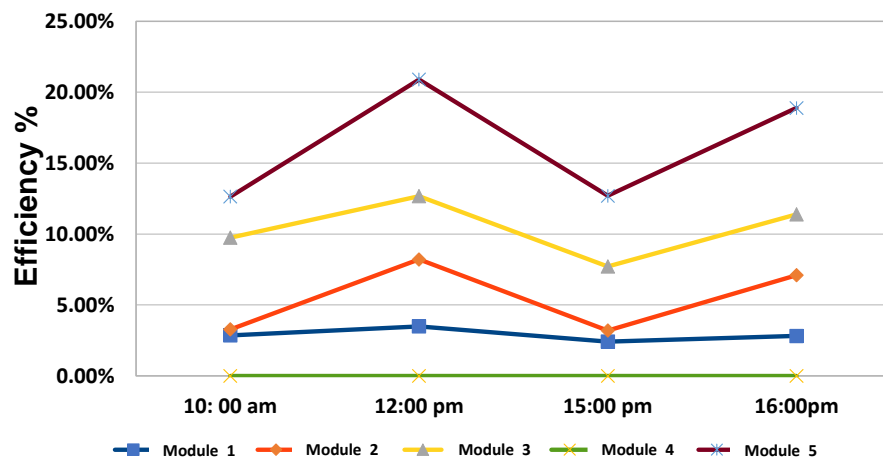
Figure 31 I-V curve Module 5



Source (Own Elaboration)

Figure 40 present the 5 modules with different irradianations. The first record was at 10:00 in the morning with a solar irradiation of 650 W/m^2 . The second record was an irradiation 1000 W/m^2 during noon, the maximum point of each module was achieved. In addition, the information in each aspect increased. The record in the irradiation at 550 W/m^2 at 15:00, losses were obtained in each result. Finally, we were able to observe a slight increase on each module at 16:00 with an irradiation at 800 W/m^2 . In general, the day has two hours of maximum irradiation, at 12:00 pm and 16:00 pm. We have a variation with respect to the course of the day, we must consider the presence of clouds, wind or objects that interfered at the time of each reading. The module with the highest efficiency is module 5, the standard average: 15% - 17% while module 3 manufactured with quality standards does not exceed 13%. However, the Shingled prototype was the module with the smallest difference in each time change and irradiation.

Figure 32 Efficiency of the modules in time zone Jocotitlan



Source (Own Elaboration)

3.3 Shadow moment test

The behavior of a photovoltaic module under different circumstances is reflected in its power and efficiency, the "Shadow Moment" test is a test that is not governed by any standardized norm, but it is a problem that affects the installations of photovoltaic modules. A large part of the companies dedicated to manufacturing carry out this type of test, carrying out two scenarios that lead to overheating and loss of current flow in the photovoltaic modules.

- Obstruction of a cell.
- Obstruction of 20% of each photovoltaic module.

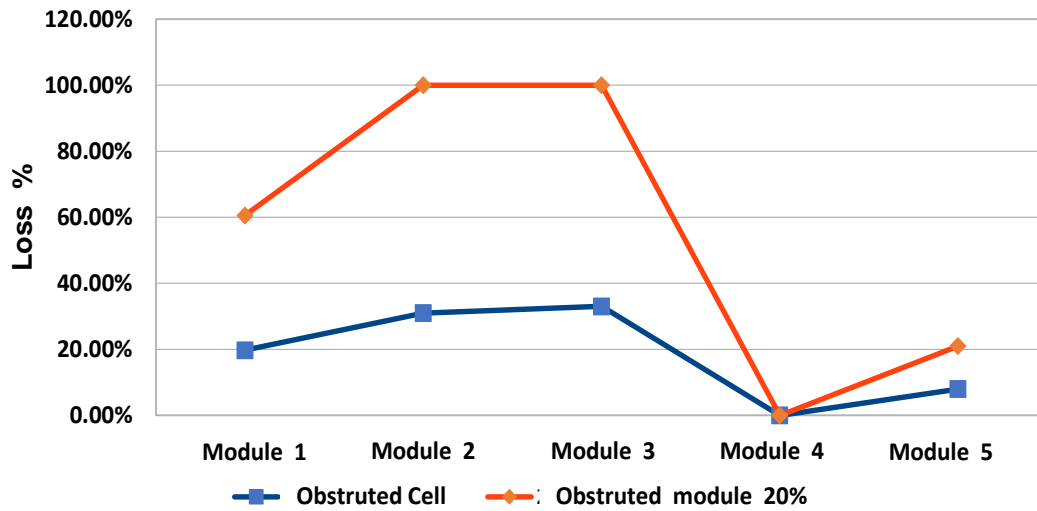
The table 2 and figure 33 shows all the modules flow in a continuous circuit connected in series, any interruption of this flow can have detrimental effects on its operation. The analyze that modules 1 and 5 connected with electrically conductive adhesives are better because they have lower percentages in the presence of a clogged cell. However, when we change the 20% shadow angle on each module, we will have a total loss in power and efficiency in module 2 and 3 (Assoa and Levrard 2020).

Table 2 Efficiencies in partial shades

No.	Module 1	Module 2	Module 3	Module 4	Module 5
Irradiation	1000 W/m^2 .	1000 W/m^2 .	1000 W/m^2 .	1000 W/m^2 .	1000 W/m^2 .
Pmax (W)	43.95 W	101.2 W	99.06 W	-	377 W
1 Cell obstruction	35.22 W -19.75 % Efic.	69.01 W -30.98 % Efic.	66.37 W -33.01 % Efic.	-	346.84 W -8 % Efic.
20 % Module obstruction	17.36 W -60.53 % Efic.	0 W 100 % Efic.	0 W -100 % Efic.	-	297.83 W -21 % Efic.

Source (Own Elaboration)

Figure 33 Cell and module obstruction test

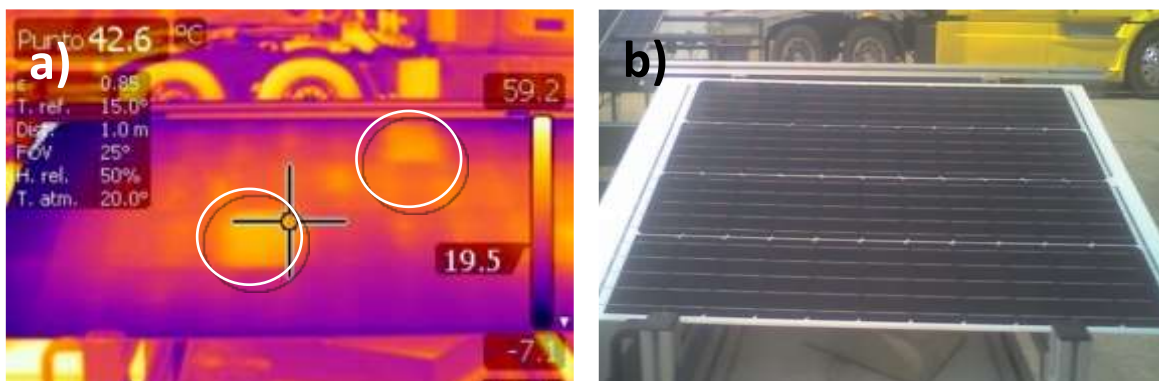


Source (Own Elaboration)

3.4 Thermographic performance

Figure 34 of module 1 shows two areas with hot spots at 43°C, this was due to excess adhesive material applied.

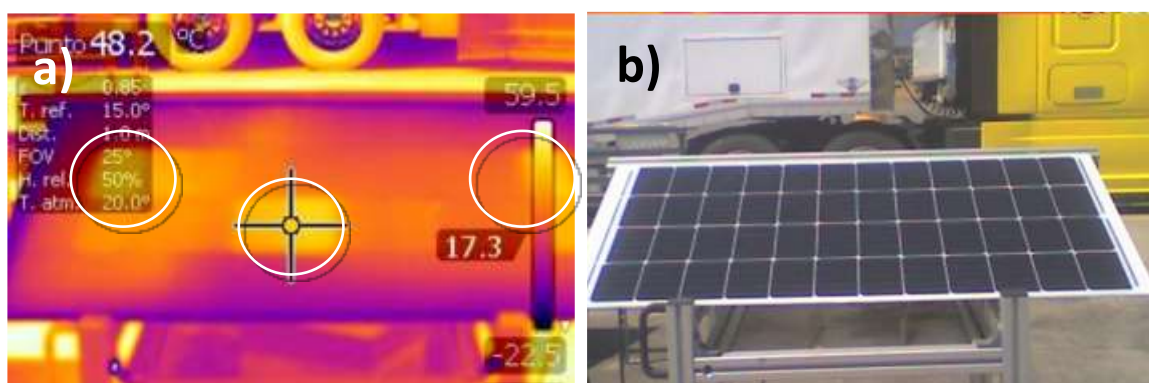
Figure 34 Thermographic testing a) with Infrared and b) without infrared image module 1



Source (Own Elaboration)

Figure 35 shown the Module 2 with infrared image with the presence of several hot spots around 48 °C, the presence of these areas marks the defects in its structure, broken cells, and micro-cracks due to the stresses exerted by the welding process.

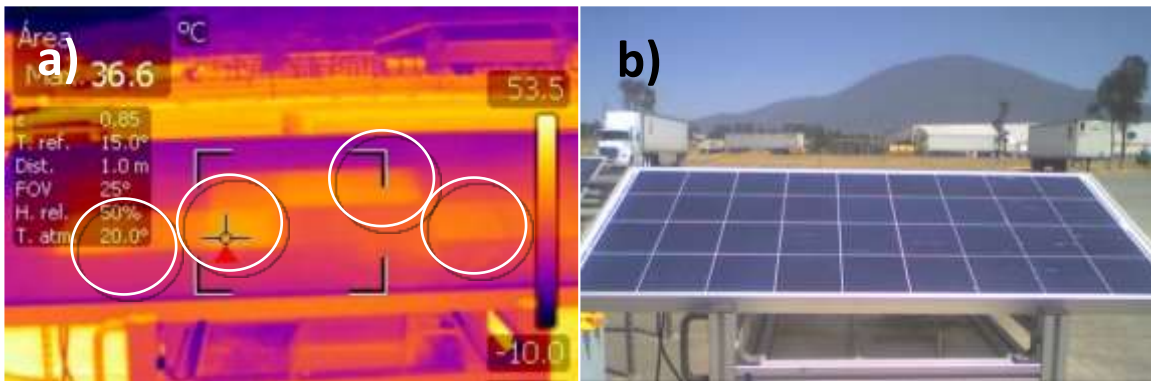
Figure 35 Thermographic testing a) with Infrared and b) without infrared image module 2



Source (Own Elaboration)

Module 3, the electroluminescence image, does not present any broken cells or micro-cracks, but since low-efficiency cells were used, the module has little resistance to temperature, as can be seen in figure 36, the areas of overheating are too many.

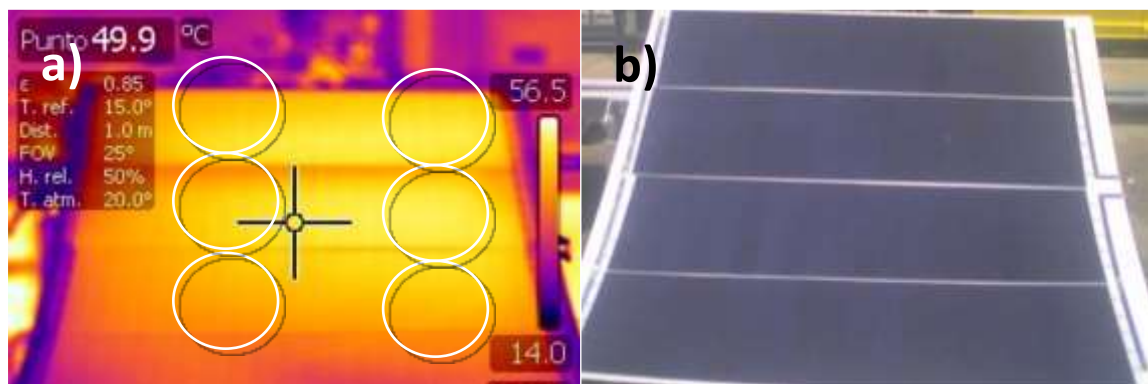
Figure 36 Thermographic testing a) with Infrared and b) without infrared image module 4



Source (Own Elaboration)

Figure 37 shows the module 4 something that in the previous tests did not present any sign of its status, however, in this thermographic test we were able to observe an increase in the operating temperature higher than the other modules. The fact of not using tempered glass and occupying a transparent EVA sheet increases the temperature because it is not dissipating heat.

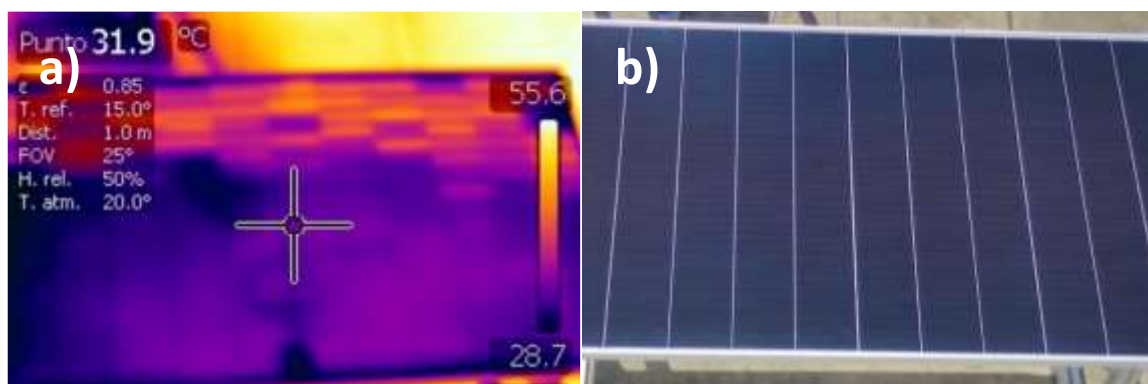
Figure 37 Thermographic testing a) with Infrared and b) without infrared image module 4



Source (Own Elaboration)

Figure 38 shown the module 5 is a reference of the objective to be achieved with the use of the electrically conductive adhesive, but it did not obtain any loss of power or efficiency.

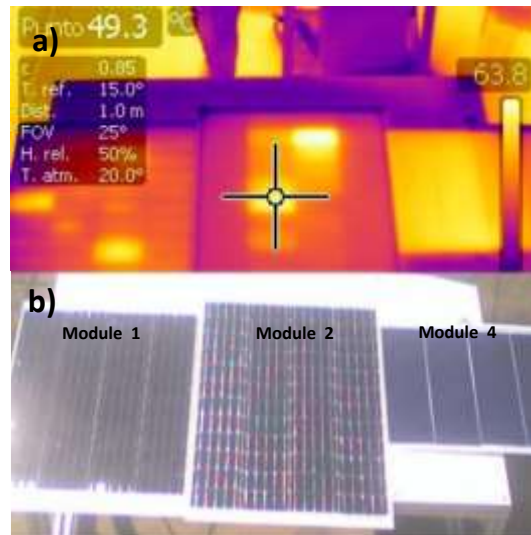
Figure 38 Thermographic testing a) with Infrared and b) without infrared image module 5



Source (Own Elaboration)

Finally, you can see in figure 39 the comparison of module 1 and 2, in which module 2 has a greater number of hot spots and module 4 has overheating throughout its entire structure.

Figure 39 Infrared image (Module 1, 2 y 4)



Source (Own Elaboration)

4. Acknowledgments

We thank the authors to TecNM-TEJJo and participating manufacturing industry.

5. Conclusions

The research conclusion is that electrically conductive adhesives improve power, efficiency, and aesthetics in the superimposition of the cells, a lower rate of broken cells, and micro-cracks, in addition to releasing mechanical stresses in temperature changes. The temperature limits efficiency losses due to partial shading in photovoltaic systems, the choice of adhesive for use in manufacturing and replacement of the welding process was Loctite 8282 adhesive. All this was achieved, but not in the proper way because, in the manufacturing process, the handling, the arrangement of the strings, and the cells are not adequate for a massive process.

The data obtained in each test reflect that the shingled technology is promising. In the inspection process, they show that electrically conductive adhesives prevent fractures of the solar cells and the generation of micro-cracks, however, it is necessary to consider that the cells used are not the correct ones for this technology, the cells with the correct screen printing for manufacturing can be seen in figure 7 to obtain a better performance on the readings carried out, the testing must be carried out in a controlled space.

6. Reference

Anderson G. L. and Macon D. J. (2021). 5-Properties of adhesives, In Woodhead Publishing Series in Welding and Other Joining Technologies, Adhesive Bonding, Second Edition, Woodhead Publishing, 2021,133-155.

<https://www.sciencedirect.com/science/article/abs/pii/B9780128199541000022?via%3Dihub>

<https://doi.org/10.1016/B978-0-12-819954-1.00002-2>

Aparicio M. P., Pelegrí J. S., Sogorb T. and Llario V. (2012). Modeling of Photovoltaic Cell Using Free Software Application for Training and Design Circuit in Photovoltaic Solar Energy, IntechOpen, 50-60.

<https://www.intechopen.com/chapters/41233>

<http://doi.org/10.5772/51925>

- Assoa Y.B. and Levrard D. (2020). A lightweight triangular building integrated photovoltaic module, *Applied Energy*, Volume 279, 115816. <https://www.sciencedirect.com/science/article/abs/pii/S0306261920312964?via%3Dihub>
<https://doi.org/10.1016/j.apenergy.2020.115816>
- Aradhana R., Mohanty S. and Nayak S. K. (2020). A review on epoxy-based electrically conductive adhesives, *International Journal of Adhesion and Adhesives*, Volume 99, 2020, 102596. <https://www.sciencedirect.com/science/article/abs/pii/S0143749620300580?via%3Dihub>
<https://doi.org/10.1016/j.ijadhadh.2020.102596>
- Beaucarne B. (2016). Materials Challenge for Shingled Cells Interconnection, *Energy Procedia*, Volume 98, 115-124. <https://www.sciencedirect.com/science/article/pii/S1876610216310487?via%3Dihub>
<https://doi.org/10.1016/j.egypro.2016.10.087>
- Dhimish M. and Holmes V. (2012). Solar cells micro crack detection technique using state-of-the-art electroluminescence imaging, *Journal of Science: Advanced Materials and Devices*, Volume 4, Issue 4, 499-508. <https://www.sciencedirect.com/science/article/pii/S2468217919302345?via%3Dihub>
<https://doi.org/10.1016/j.jsamd.2019.10.004>
- Elsayed H., Picicco M., Dasan A., Kraxner J., Galusek D. and Bernardo E. (2020). Glass powders and reactive silicone binder: Application to digital light processing of bioactive glass-ceramic scaffolds, *Ceramics International*, Volume 46, Issue 16, Part A, 25299-25305. <https://www.sciencedirect.com/science/article/pii/S0272884220319957?via%3Dihub>
<https://doi.org/10.1016/j.ceramint.2020.06.323>
- Guo Z., Lu W., Zhang Y., Zhou J., and Sun D., (2023) MXene fillers and silver flakes filled epoxy resin for new hybrid conductive adhesives, *Ceramics International*, Volume 49, Issue 8, 2054-12060. <https://www.sciencedirect.com/science/article/abs/pii/S0272884222044509?via%3Dihub>
<https://doi.org/10.1016/j.ceramint.2022.12.055>
- Li L. and Morris J. E. (1997). Electrical conduction models for isotropically conductive adhesive joints," in *IEEE Transactions on Components, Packaging, and Manufacturing Technology: Part A*, Vol. 20, 1, 3-8. <https://ieeexplore.ieee.org/document/558537>
<https://doi.org/10.1109/95.558537>
- Malik M. H., Grosso G., Zangl H., Binder A. and Roshanghias A. (2021). Flip Chip integration of ultra-thinned dies in low-cost flexible printed electronics; the effects of die thickness, encapsulation and conductive adhesives, *Microelectronics Reliability*, Volume 123, 2021, 114-204. <https://www.sciencedirect.com/science/article/pii/S0026271421001700?via%3Dihub>
<https://doi.org/10.1016/j.microrel.2021.114204>
- Oh W., Park J., Jeong C., Park J., Yi J. and Lee J. (2020). Design of a solar cell electrode for a shingled photovoltaic module application, *Applied Surface Science*, Volume 510, 145420. <https://www.sciencedirect.com/science/article/abs/pii/S0169433220301768?via%3Dihub>
<https://doi.org/10.1016/j.apsusc.2020.145420>
- Pander S. H. and Schulze M. E. (2014). Mechanical Modelling of Electrically Conductive Adhesives for Photovoltaic Applications, Conference: 29th European Photovoltaic Solar Energy Conference and Exhibition, 3399 – 3406. <https://userarea.eupvsec.org/proceedings/EU-PVSEC-2014/5DV.3.39/>
<https://doi.org/10.4229/EUPVSEC20142014-5DV.3.39>
- Saeedi I. A., Chalashkanov N., Dissado L. A., Vaughan A.S. and Andritsch T. (2022). The nature of the gamma dielectric relaxation in diglycidyl ether Bisphenol-A (DGEBA) based epoxies, *Polymer*, Volume 249, 124861. <https://www.sciencedirect.com/science/article/abs/pii/S0032386122003482?via%3Dihub>
<https://doi.org/10.1016/j.polymer.2022.124861>

Sharma D., Mehra R. and Raj B. (2021). Comparative analysis of photovoltaic technologies for high efficiency solar cell design, *Superlattices and Microstructures*, Volume 153, 106861. <https://www.sciencedirect.com/science/article/abs/pii/S0749603621000598?via%3Dihub>
<https://doi.org/10.1016/j.spmi.2021.106861>

Springer M. and Bosco N. (2020). "Linear viscoelastic characterization of electrically conductive adhesives used as interconnect in photovoltaic modules", *Progress in Photovoltaics: Research and Applications*, Vol. 28, 7, 659-681. <https://onlinelibrary.wiley.com/doi/abs/10.1002/pip.3257>
<https://doi.org/10.1002/pip.3257>

Svarc J. (2020, March 20). "Panel Solar Construction. *Clean Energy Review* [Online blog] <https://www.cleanenergyreviews.info/blog/solar-panel-components-construction>

Tonini D., Cellere G., Bertazzo M., Fecchio A., Cerasti L., and Galiazzo M. (2018). Shingling Technology For Cell Interconnection: Technological Aspects and Process Integration, *Energy Procedia*, Volume 150, 36-43. <https://www.sciencedirect.com/science/article/pii/S1876610218305502?via%3Dihub>
<https://doi.org/10.1016/j.egypro.2018.09.010>

Xiao G., Liu E., Jin T., Shu S., Wang Z., Yuan G., and Yang X. (2017). Mechanical properties of cured isotropic conductive adhesive (ICA) under hygrothermal aging investigated by micro-indentation, *International Journal of Solids and Structures*, Volumes 122–123, 81-90. <https://www.sciencedirect.com/science/article/pii/S0020768317302597?via%3Dihub>
<https://doi.org/10.1016/j.ijsolstr.2017.06.003>